

## Laser direct patterning of AgNW/CNT hybrid thin films



Ji-Wook Yoon<sup>a,b</sup>, Won Seok Chang<sup>a,b,\*</sup>, Sung Hak Cho<sup>a,b,\*\*</sup>

<sup>a</sup> Nano-Convergence Mechanical Systems Research Division, Korea Institute of Machinery and Materials (KIMM), 156 Gajeongbuk-Ro, Yuseong-gu, Daejeon 305-343, South Korea

<sup>b</sup> Department of Nano-Mechatronics, Korea University of Science and Technology (UST), 217 Gajeong-Ro, Yuseong-gu, Daejeon 305-350, South Korea

### ARTICLE INFO

#### Article history:

Received 31 October 2014

Received in revised form

5 March 2015

Accepted 3 April 2015

#### Keywords:

Laser direct patterning

AgNW/CNT

Femtosecond laser

Transparent electrode

### ABSTRACT

A hybrid material composed of silver nanowires (AgNWs) and carbon nanotubes (CNTs) is investigated by a laser direct patterning method. A femtosecond laser system with a wavelength of 1027 nm and a pulse width of 380 fs is applied for the patterning of AgNW/CNT hybrid film. The Gaussian and square quasi-flat-top beam profiles are used for the patterning lines. The laser fluence and overlapping rate were optimized for patterning at 67.9 mJ/cm<sup>2</sup> and 70%, respectively. The patterned AgNW/CNT film is evaluated using an optical microscope and scanning electron microscope. The partially ablated area of AgNW/CNT films around the patterned line is observed and discussed. The measurement results explain that the uniformity of the laser beam profile and the beam shape are key factors for development of AgNW/CNT films with fine edges.

© 2015 Elsevier Ltd. All rights reserved.

### 1. Introduction

Recently, conductive materials for transparent electrodes have gathered much attention for application in optoelectronic devices including flat panel displays, organic light emitting diodes, flexible electronics, and touch panels. Doped oxides, such as indium tin oxide (ITO) and fluorine tin oxide (FTO), have been widely used for transparent electrodes due to their good transparency in the visible spectrum range and low sheet resistance [1–4]. Electronics manufacturers have investigated alternative materials to replace the metal oxides in transparent electrodes such as carbon nanotubes (CNTs), graphene, and metallic nanowires, because doped oxides have disadvantages including brittleness and high cost [1,4–9]. In the research, Takuno et al. have reported that silver nanowires (AgNWs) and CNT hybrid conductive materials have excellent properties for transparent electrodes [10]. In AgNW/CNT hybrid films, because the CNTs form bridges between the AgNWs, they can obtain high conductivity and low sheet resistance for optoelectronic devices including flexible applications.

Conventional electrode patterning methods on substrate surfaces require various expensive equipments and multiple steps in the

process including photolithography, baking, and chemical wet etching processes. Compared with the photolithography process, laser direct patterning has several advantages such as non-contact dry etching, maskless patterning, single-step patterning, and eco-friendly processes [11–15]. There have been numerous investigations about the laser direct patterning of transparent electrode materials. Liu et al. reported the maskless patterning of an Al-cathode for organic light emitting diodes using a Q-switched nanosecond laser [11]. Kalita et al. reported a femtosecond laser ablation result for graphene film cutting; their homogenous microribbon structures were fabricated without using resists or other material [12]. Chen et al. demonstrated programmable patterning of graphene in order to create patterns using femtosecond laser direct patterning on graphene oxide films [13]. Tseng et al. used an ultraviolet nanosecond laser to scribe a PEDOT:PSS [(poly(3,4-ethylenedioxythiophene):poly(4-styrenesulfonate))] film surface in order to develop touch panel screen electrodes [14]. Lin et al. presented laser patterning of CNT films on polymer substrates using a nanosecond laser; by controlling the patterning speed and pulse energy, the CNT films were patterned as electrodes for touch panel applications [15]. Many studies have undertaken regarding electrode patterning using laser direct patterning techniques with various novel materials; however, laser direct patterning for AgNW/CNT materials have not yet been reported.

Femtosecond laser has been considered as micromachining tool for various functional materials due to their advantages of precise ablation with minimized thermal influence [16]. Although femtosecond lasers show great performance when used to ablate material, there is a limitation to improve the quality near the laser irradiated area due to the energy distribution of the laser

\* Corresponding author at: Nano-Convergence Mechanical Systems Research Division, Korea Institute of Machinery and Materials (KIMM), 156 Gajeongbuk-Ro, Yuseong-gu, Daejeon 305-343, South Korea. Tel.: +82 42 868 7134.

\*\* Corresponding author at: Nano-Convergence Mechanical Systems Research Division, Korea Institute of Machinery and Materials (KIMM), 156 Gajeongbuk-Ro, Yuseong-gu, Daejeon 305-343, South Korea. Tel.: +82 42 868 7077.

E-mail addresses: [paul@kimm.re.kr](mailto:paul@kimm.re.kr) (W.S. Chang), [shcho@kimm.re.kr](mailto:shcho@kimm.re.kr) (S.H. Cho).

beam. In this study, we patterned AgNW/CNT film with fine edge shape deposited onto glass substrate using a femtosecond laser system with a beam shaping technique. The technique used in this experiment could be useful for flexible display applications. A femtosecond laser was used to remove AgNW/CNT films selectively using the Gaussian and square quasi-flat-top beam profiles via a scanner system. The Gaussian beam and square quasi-flat-top beam profile were measured by beam profiler (LASERCAM II 1/2). The spot overlapping rate and machining threshold for the laser direct patterning were calculated to achieve optimized patterning conditions. The experimental results were evaluated using an optical microscope and scanning electron microscope (SEM). The laser direct patterning results and the patterned shapes of the AgNW/CNT films are discussed.

## 2. Experiments

A schematic diagram of the experimental set up is presented in Fig. 1. A diode pumped Yb:KYW thin disk femtosecond laser system at 1027 nm wavelength with a pulse width of 380 fs was used to pattern the AgNW/CNT. Depending on the experiment arrangement, the Gaussian beam profile or square quasi-flat-top beam profile was employed. Images of the energy distribution of the Gaussian beam and square quasi-flat-top beam profiles are depicted in Fig. 2. A laser beam with the Gaussian beam profile was delivered onto the sample through a beam expander with magnitude of  $3\times$ . The square quasi-flat-top laser beam profile was constructed using optic components including adjustable slit in

microscale and plano-convex lens. An  $F$ -theta lens with focal length of 100 mm and a galvanometric scanner were used to control the beam path on substrate.

The SEM image of the AgNW/CNT films deposited on a glass substrate is presented in Fig. 3. The hybrid film, which consisted of the AgNWs (diameter=25 nm, length=25  $\mu\text{m}$ ) and CNTs (diameter=3 nm, length=5  $\mu\text{m}$ ), was prepared on a soda-lime glass substrate. The thickness of the AgNW/CNT film and the glass substrate were 60 nm and 700  $\mu\text{m}$ , respectively. The transparency in the visible wavelength range was 81% with a sheet resistance of 20  $\Omega/\text{sq}$ .

The overlapping rate of laser irradiation is one of an important parameters for laser patterning process because a line pattern is created with a large number of ablated spots. The overlapping rate depends on the scanning speed and repetition rate of laser pulse. In this experiment, the repetition rate of the laser pulse was fixed at 100 kHz and the overlapping rate was managed through changing the scanning speed. The overlapping rate was obtained using the following equation.

$$\text{Overlapping rate} = \left(1 - \frac{V}{wF}\right) \times 100\% \quad (1)$$

where  $w$  is the focused beam diameter,  $V$  is the laser scanning speed, and  $F$  is the laser repetition rate.

## 3. Results and discussions

The surface morphologies of the ablated areas were produced by single pulse femtosecond irradiation with the Gaussian beam profile at laser fluence values ranging from 9.7  $\text{mJ}/\text{cm}^2$  to 70.8  $\text{mJ}/\text{cm}^2$

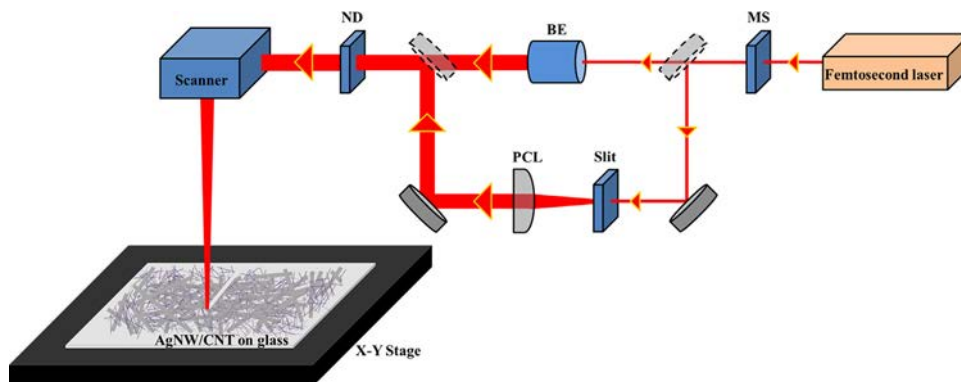


Fig. 1. Schematic of the experimental setup. ND: Neutral density filter, PCL: Plano-convex lens, MS: Mechanical shutter, BE: Beam expander.

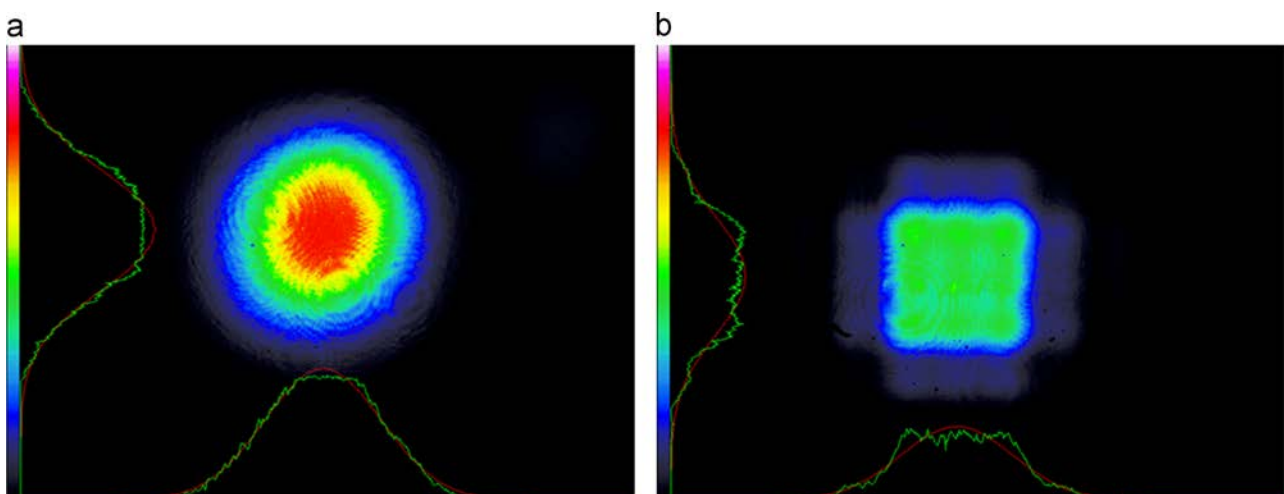


Fig. 2. Images of (a) the Gaussian and (b) square quasi-flat-top beam profile.

$\text{cm}^2$ . Fig. 4 shows images of the laser fluences of  $13.6 \text{ mJ}/\text{cm}^2$ ,  $47.7 \text{ mJ}/\text{cm}^2$ ,  $57.8 \text{ mJ}/\text{cm}^2$ , and  $67.9 \text{ mJ}/\text{cm}^2$ . When the laser fluence was  $13.6 \text{ mJ}/\text{cm}^2$ , the AgNW/CNT was not completely removed, but ablation occurred for the first time. When the laser fluence was

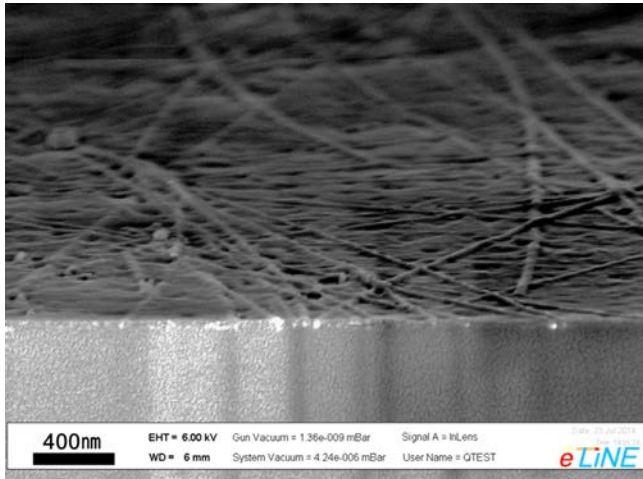


Fig. 3. SEM quarter view image of the AgNW/CNT film deposited on a glass substrate.

$47.7 \text{ mJ}/\text{cm}^2$  or more, as seen in Fig. 4(b), the totally ablated area was observed at the center of the irradiated area. In Fig. 4(c and d), the partially ablated area decreased and the clearly ablated area increased. When the laser beam was irradiated with fluence more than  $67.9 \text{ mJ}/\text{cm}^2$ , damage to the glass substrate appeared, and engraved marks were also observed on the center of the irradiated region. Compared to the experiment for CNT film ablation, CNT was ablated for the first time at a laser fluence of  $50 \text{ mJ}/\text{cm}^2$ . From this experimental result, we concluded that CNT was not ablated when the laser fluence of  $13.6 \text{ mJ}/\text{cm}^2$  whereas AgNW ablation began. For this reason, we determined that the interaction between the laser pulse and AgNW/CNT film began at a fluence of  $13.6 \text{ mJ}/\text{cm}^2$ , i.e., the threshold value ( $F_{th}$ ).

The SEM images of the patterned lines are presented in Fig. 5. Because the substrate was damaged when fluence values greater than  $5F_{th}$  were used, line patterning was performed at a laser pulse repetition rate of  $100 \text{ kHz}$  with a fluence of  $5F_{th}$ . All the parameters for the patterning except scanning speed were fixed. The overlapping rate calculated using Eq. (1) was controlled using the scanning speed with values of 30%, 50%, 70%, and 90%. When the overlapping rate of the laser beam spot was 30%, the residuals were not completely removed between the ablated spots as seen in Fig. 5(a). Fig. 5(b) illustrates that the clearly ablated areas are connected in a line, but the line edge remained in a wave shape. In Fig. 5(c and d), a straight line form was observed with the

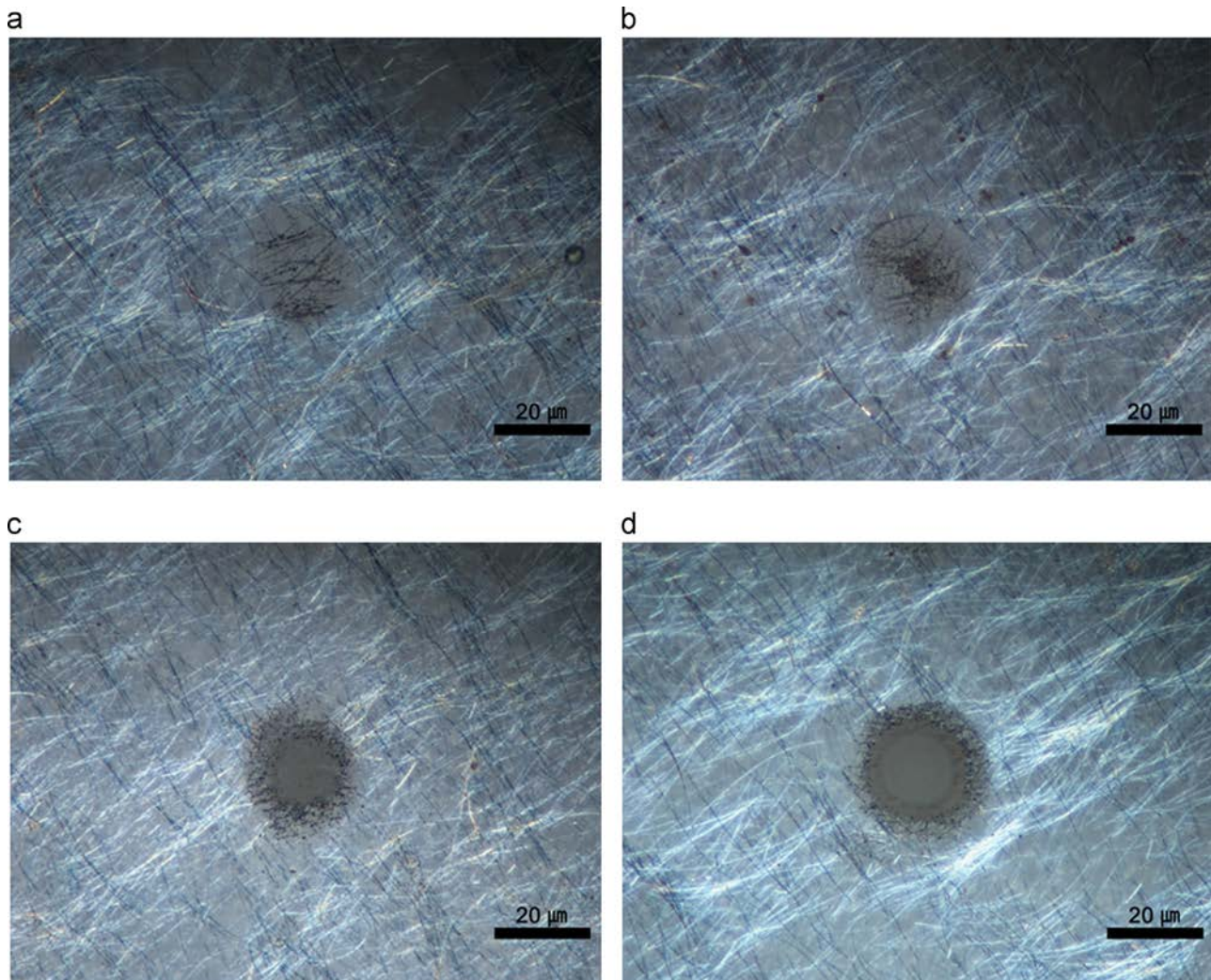


Fig. 4. Optical microscope images of AgNW/CNT morphology after a single pulse irradiation with fluences of (a)  $13.6 \text{ mJ}/\text{cm}^2$  ( $F_{th}$ ), (b)  $47.7 \text{ mJ}/\text{cm}^2$  ( $3.5F_{th}$ ), (c)  $57.8 \text{ mJ}/\text{cm}^2$  ( $4.3F_{th}$ ), and (d)  $67.9 \text{ mJ}/\text{cm}^2$  ( $5.0F_{th}$ ), respectively.

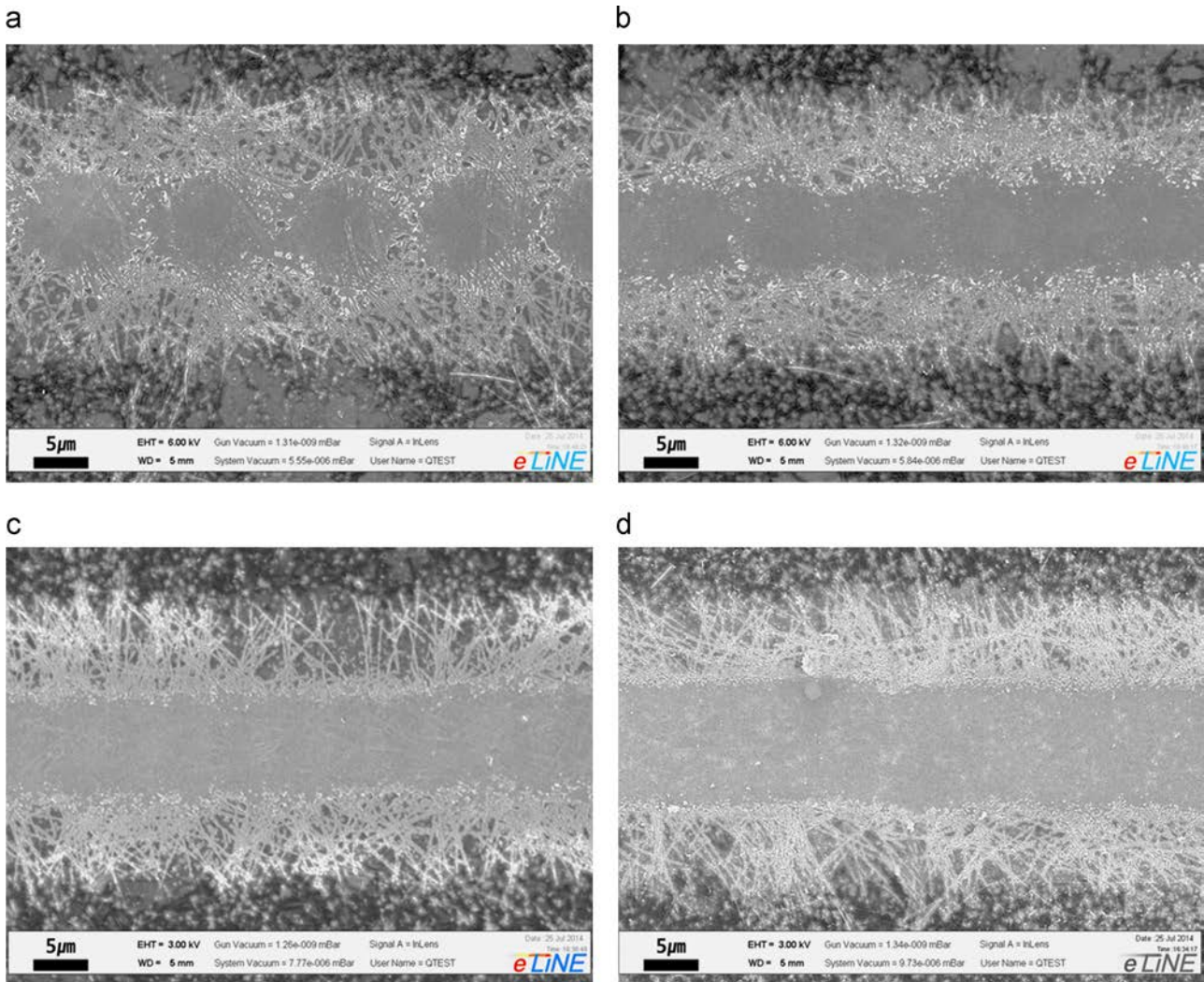


Fig. 5. Images of AgNW/CNT ablated line with an overlapping rate of (a) 30%, (b) 50%, (c) 70%, and (d) 90%.

overlapping rates of 70% and 90%. The results demonstrated that the width of the partially ablated area, which was limited to diameter of the focused beam, was similar for all results; however, the clearly ablated region increased slightly as a result of the increasing overlapping rate. From the measurement results, structuring the partially ablated region was not much influenced by the overlapping rate, but it was affected by the focused beam size and energy distribution. In consideration of the laser repetition rate, the scanning speed and the interaction time scale between the material and femtosecond laser pulse, we concluded that the patterning process was carried out with a minimal thermal effect.

When femtosecond pulses are irradiated on the AgNW/CNT film, uneven shape appears at the edge of the ablated area. Possible explanation for the shape of the line edge is the threshold difference of the AgNWs and CNTs. For the laser patterning of the transparent conductive film with a single material, the ablation threshold of thin film was a less critical factor for developing fine edges because the clearly ablated area was resulted from difference of the ablation threshold values between the conductive film and substrate. However, using the laser direct patterning for the hybrid material film, which composed of more than two materials maintaining their own characteristics, the ablation threshold values must be considered between not only the hybrid material film and substrate, but also each material. For the same reason, although the AgNW/CNT film had a significantly lower ablation

threshold than the glass substrate, the edge of the patterned line had rugged shape due to the threshold differences between the AgNWs and CNTs.

For optoelectronic devices, well-defined electrode edges are important because irregularly patterned edges can cause malfunctions or low efficiency in the devices. In our experiment, the result of the line patterning on the AgNW/CNT film with the Gaussian beam profile revealed that it had limitations in improving the edge quality of the ablated line for the AgNW/CNT film patterning. Therefore, in order to obtain a fine line edge, the AgNW/CNT film was ablated using the square quasi-flat-top beam profile. The laser beam was expanded using a plano-convex lens, and the beam size was adjusted using the X–Y slit in order to develop the square shape of the quasi-flat-top beam profile. The overlapping rate and fluence were 70% and 5fth, respectively.

Fig. 6 presents the line patterning results using the Gaussian beam profile. In Fig. 6(a), the deformation of the AgNW/CNT film was observed along the patterned line. Furthermore, many particles and craters were observed in the partially ablated region where the AgNWs appeared, as seen in Fig. 6(b). Fig. 6(c and d) presents the patterning results using the square quasi-flat-top beam profile. The measurement results exhibited a fine line curve and significantly less uneven area near the patterned region. In comparison with Fig. 6(b), the irregularly ablated marks with particles and craters remained in Fig. 6(d), but they were

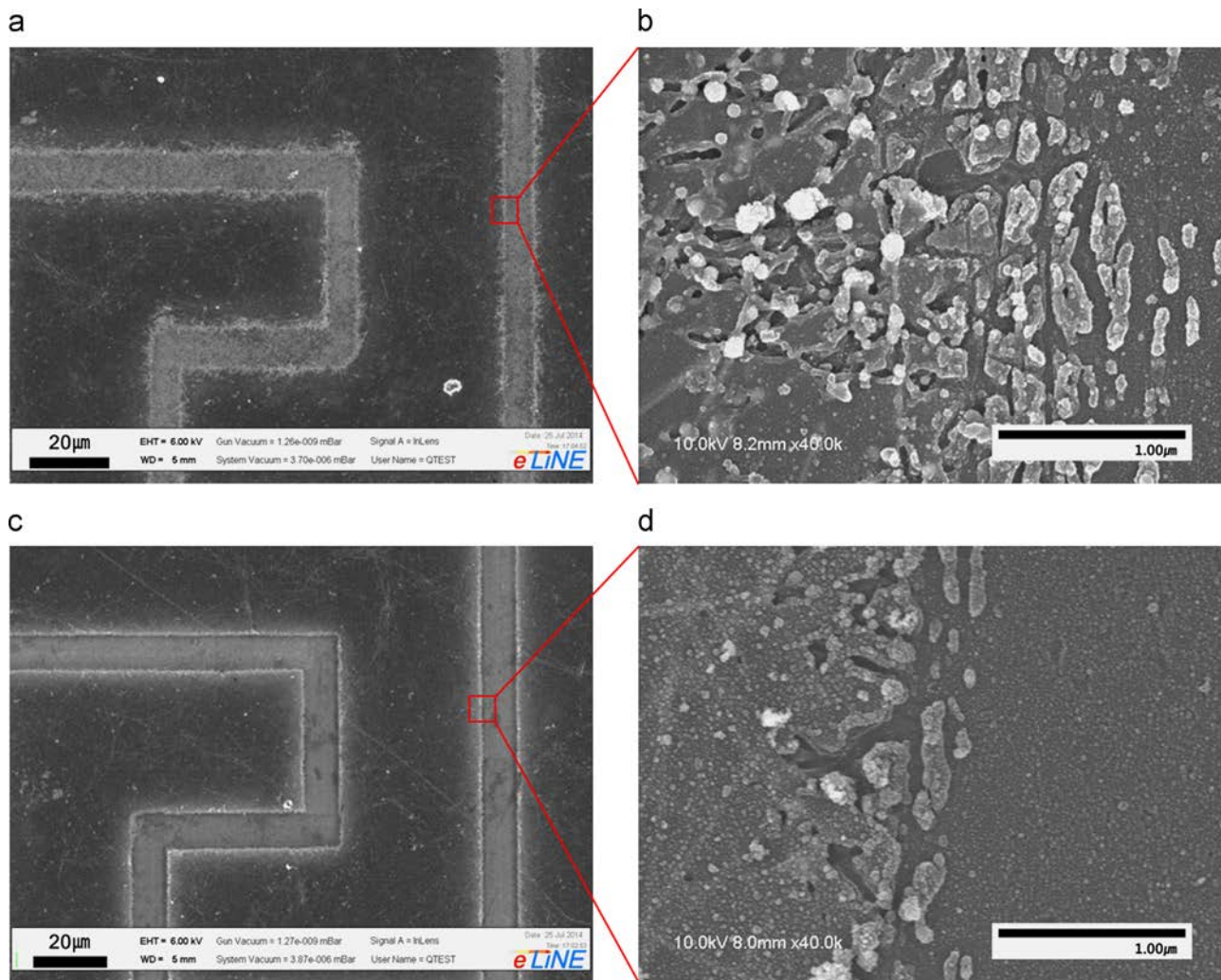


**Fig. 6.** SEM images of the patterned lines using laser beam with the Gaussian and square quasi-flat-top beam profile: (a) patterned line with the Gaussian beam profile, (b) magnified image of (a), (c) patterned line with the square quasi-flat-top beam profile, and (d) magnified image (c).

substantially decreased. Additionally, the widths of the partially ablated area were measured. Those were  $12\ \mu\text{m}$  in Fig. 6(b), and  $2\ \mu\text{m}$ , as shown in Fig. 6(d). Although deformation of the AgNW/CNT near the patterned line was observed in both samples, the results by the square quasi-flat-top beam profile showed a reduced ablated area by six times compared to the Gaussian beam profile results.

The schematic and its fabricated image of a touch panel electrode are presented in Fig. 7. The AgNW/CNT electrode was obtained using the qualified parameters for the laser fluence ( $5F_{th}$ ) and overlapping rate (70%) with the square quasi-flat-top beam profile. The size of the square quasi-flat-top beam was  $18 \times 18\ \mu\text{m}$ , and multiple parallel lines with  $15\ \mu\text{m}$  intervals were designed for the patterning of the electrode. In Fig. 7(a), the black areas indicate the ablated region with the laser direct patterning, and the white squares are unablated regions where the AgNW/CNT remained. The size of the obtained pattern was  $23\ \text{mm} \times 39.5\ \text{mm}$ , and the electrodes were patterned with approximately  $0.5\ \text{mm} \times 35\ \text{mm}$ . Fig. 7(b) presents the photograph images of the electrode developed using the femtosecond laser direct patterning with the square quasi-flat-top beam profile. After patterning the electrode, the resistance between electrodes was measured, and it was confirmed that the AgNW/CNT transparent electrode was successfully isolated.

The Gaussian and square quasi-flat-top beam profile were used to develop the AgNW/CNT line pattern with parameters of 70%

overlapping rate and laser fluence of  $5F_{th}$ . When the square quasi-flat-top beam profile is compared with the Gaussian beam profile, the AgNW/CNT film fabricated using the square quasi-flat-top beam profile had a finer edge shape and less partially ablated areas near the patterned line. The magnified morphology of the patterned line applied using the Gaussian and square quasi-flat-top beam profiles revealed that the uniformity of the beam energy distribution and the shape of the focused beam were key factors for line patterning of the AgNW/CNT hybrid materials with fine edge qualities.

#### 4. Conclusion

It was a challenging task as it was the first demonstration, to the best of our knowledge, of AgNW/CNT hybrid film using a femtosecond laser direct patterning technique and given the lack of references. In our experiment, laser direct patterning results using the Gaussian beam profile and quasi-flat-top beam profile were compared. Due to the limitation of the enhancement of the edge quality near the ablation area in case of laser direct patterning with the Gaussian beam profile, we used quasi-flat-top beam profile to pattern lines with fine edge. Compared to the Gaussian beam profile results, the partially ablated area near the patterned line was reduced by nearly six times when the square quasi-flat-

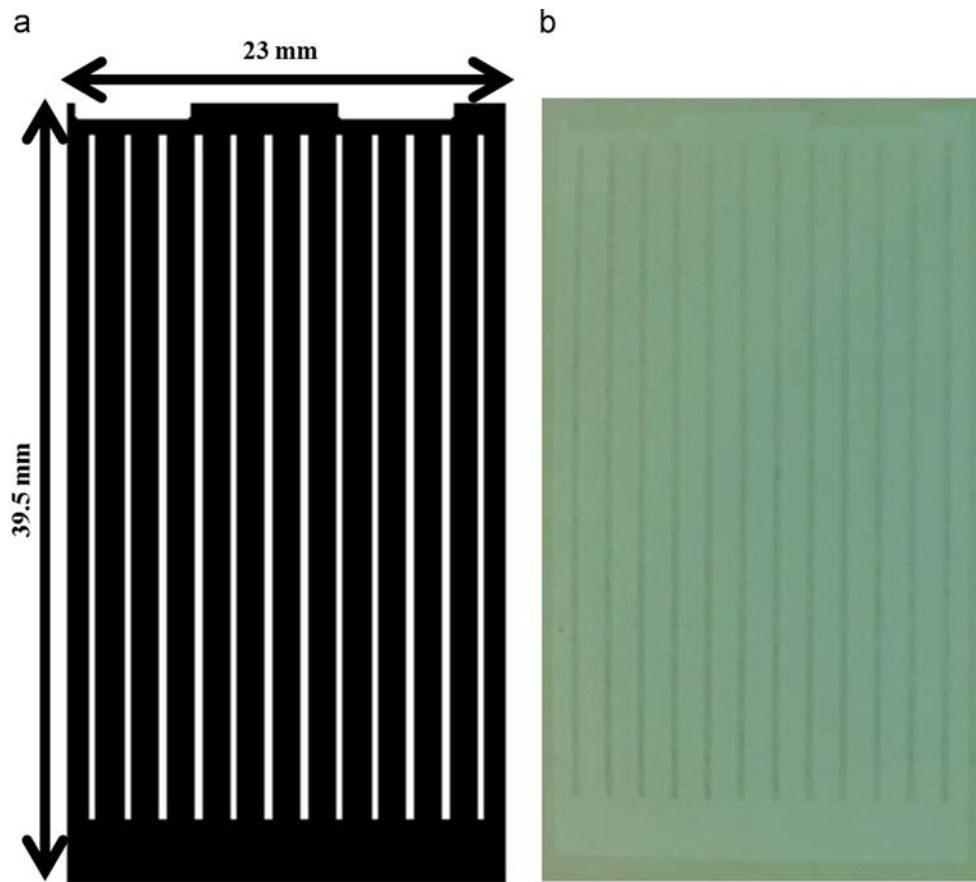


**Fig. 7.** Images of the touch panel electrodes: (a) schematic of the electrode pattern and (b) photographic image of the AgNW/CNT electrode developed using laser direct patterning.

top beam profile was used. As a result of the difference in the uniformity and the focused beam shape between both beam profiles, the ablation morphology around the AgNW/CNT was observed to be different. These current experiment results demonstrated the potential of AgNW/CNT hybrid film direct patterning using ultrafast laser.

### Acknowledgments

This work was partially supported by Nano-Material Technology Development Program (Green Nano Technology Development Program) through the National Research Foundation of Korea (NRF) funded by the Ministry of Education, Science and Technology (NRF-2011-0020506) and by the Center for Advanced Meta-Materials (CAMM) funded by the Ministry of Science, ICT and Future Planning as Global Frontier Project (CAMM- No. 2014M3A6B3063707).

### References

- [1] Kumar A, Zhou C. The race to replace tin-doped indium oxide: which material will win? *ACS Nano* 2010;4(1):11–4.
- [2] Yoo B, Kim KJ, Bang SY, Ko MJ, Kim K, Park NG. Chemically deposited blocking layers on FTO substrates: effect of precursor concentration on photovoltaic performance of dye-sensitized solar cells. *J Electroanal Chem* 2010;638(1):161–6.
- [3] Tachan Z, Ruhle S, Zaban A. Dye-sensitized solar tubes: a new solar cell design for efficient current collection and improved cell sealing. *Sol Energy Mater Sol Cells* 2010;94(2):317–22.
- [4] Hecht DS, Hu L, Irvin G. Emerging transparent electrodes based on thin films of carbon nanotubes, graphene, and metallic nanostructures. *Adv Mater* 2011;23(13):1482–513.
- [5] Wu Z, Chen Z, Du X, Logan JM, Sippel J, Nikolou M, et al. Transparent, conductive, carbon nanotube films. *Science* 2004;305(5688):1273–6.
- [6] Eda G, Fanchini G, Chhowalla M. Large-area ultrathin films of reduced graphene oxide as a transparent and flexible electronic material. *Nat Nanotechnol* 2008;3:270–4.
- [7] Wassei JK, Kaner RB. Graphene a promising transparent conductor. *Mater Today* 2010;13(3):52–9.
- [8] Lee JY, Connor ST, Cui Y, Peumans P. Solution-processed metal nanowire mesh transparent electrodes. *Nano Lett* 2008;8(2):689–92.
- [9] Tokuno T, Nogi M, Karakawa M, Jiu J, Nge TT, Aso Y, et al. Fabrication of silver nanowire transparent electrodes at room temperature. *Nano Res* 2011;4(12):1215–22.
- [10] Tokuno T, Nogi M, Jiu J, Suganuma K. Hybrid transparent electrodes of silver nanowires and carbon nanotubes: a low-temperature solution process. *Nano Express* 2012;7:281–7.
- [11] Liu C, Zhu G, Liu D. Patterning cathode for organic light-emitting diode by pulsed laser ablation. *Displays* 2008;29(5):536–40.
- [12] Kalita G, Qi L, Namba Y, Wakita K, Umeno M. Femtosecond laser induced micropatterning of graphene film. *Mater Lett* 2011;65(11):1569–72.
- [13] Chen H Y, Han D, Tian Y, Shao R, Wei S. Mask-free and programmable patterning of graphene by ultrafast laser direct writing. *Chem Phys* 2014;430:13–7.
- [14] Tseng SF, Hsiao WT, Huang KC, Huang KC. Electrode patterning on PEDOT:PSS thin films by pulsed ultraviolet laser for touch panel screens. *Appl Phys A* 2013;112(1):41–7.
- [15] Lin HK, Lin RC, Li CH. Etching processes of transparent carbon nanotube thin films using laser technologies. *Thin Solid Films* 2010;518(24):7253–7.
- [16] Chichkov BN, Momma C, Nolte S, Alvensleben FV, Tünnermann A. Femtosecond, picosecond and nanosecond laser ablation of solid. *Appl Phys A* 1996;63(2):109–15.